# High altitude ion heating observed by the Cluster spacecraft

MARTIN WAARA

# High altitude ion heating observed
# by the Cluster spacecraft

Martin Waara

Doctoral Thesis
Kiruna, Sweden, 2011

**Abstract**

This thesis deals with heating of outflowing oxygen ions at high altitude above the polar cap using data from the Cluster spacecraft. Ionospheric plasma may flow up from the ionosphere but at velocities which are low enough that the ions are still gravitationally bound. For the ions to overcome gravity, further acceleration is needed. The cusp/polar cap is an important source of outflowing oxygen ions. In the cusp/polar cap, transverse heating is more common than field-aligned acceleration through a magnetic field-aligned electric field. It is thus believed that transverse heating of ions is important for ion outflow and one of the probable explanations for transverse heating is wave-particle interaction.

A general conclusion from our work on high altitude oxygen ion energization is that ion energization and outflow occur in the high altitude cusp and mantle. The particles are often heated perpendicularly to the geomagnetic field and resonant heating at the gyrofrequency is most of the time intense enough to explain the observed $O^+$ energies measured in the high altitude (8-15 Earth radii, $R_E$) cusp/mantle region of the terrestrial magnetosphere. The observed average waves can explain the observed average $O^+$ energies. At lower altitude only a few percent of the observed spectral density around the oxygen gyrofrequency needs to be in resonance with the ions to obtain the measured $O^+$ energies. A difference as compared to low altitude measurements is that we must assume that almost all wave activity is due to waves which can interact with the ions, and of these we assume 50 % to be left-hand polarized. We also have shown a clear correlation between temperature and wave intensity at the gyrofrequency at each measurement point. We have described the average wave intensity and corresponding velocity diffusion coefficients as a function of altitude in a format convenient for modelers.
Furthermore we have shown that the wave activity observed in this high altitude region is consistent with Alfvén waves, and inconsistent with static structures drifting past the spacecraft. We have also shown how large the variability of the observed spectral densities is, and how sporadic the waves typically are. Based on three cases we have found that the regions with enhanced wave activity and increased ion temperature are typically many ion gyro radii in perpendicular extent.

# High altitude ion heating observed
# by the Cluster spacecraft

Martin Waara

# Abstract

This thesis deals with heating of outflowing oxygen ions at high altitude above the polar cap using data from the Cluster spacecraft. Ionospheric plasma may flow up from the ionosphere but at velocities which are low enough that the ions are still gravitationally bound. For the ions to overcome gravity, further acceleration is needed. The cusp/polar cap is an important source of outflowing oxygen ions. In the cusp/polar cap, transverse heating is more common than field-aligned acceleration through a magnetic field-aligned electric field. It is thus believed that transverse heating of ions is important for ion outflow and one of the probable explanations for transverse heating is wave-particle interaction.

A general conclusion from our work on high altitude oxygen ion energization is that ion energization and outflow occur in the high altitude cusp and mantle. The particles are often heated perpendicularly to the geomagnetic field and resonant heating at the gyrofrequency is most of the time intense enough to explain the observed $O^+$ energies measured in the high altitude ($8 - 15$ Earth radii, $R_E$) cusp/mantle region of the terrestrial magnetosphere. The observed average waves can explain the observed average $O^+$ energies. At lower altitude only a few percent of the observed spectral density around the oxygen gyrofrequency needs to be in resonance with the ions to obtain the measured $O^+$ energies. A difference as compared to low altitude measurements is that we must assume that almost all wave activity is due to waves which can interact with the ions, and of these we assume 50 % to be left-hand polarized. We also have shown a clear correlation between temperature and wave intensity at the gyrofrequency at each measurement point. We have described the average wave intensity and corresponding velocity diffusion coefficients as a function of altitude in a format convenient for modelers.

Furthermore we have shown that the wave activity observed in this high altitude region is consistent with Alfvén waves, and inconsistent with static structures drifting past the spacecraft. We have also shown how large the variability of the observed spectral densities is, and how sporadic the waves typically are. Based on three cases we have found that the regions with enhanced wave activity and increased ion temperature are typically many ion gyro radii in perpendicular extent.

# Sammanfattning

Avhandlingen behandlar upphettningen av utflödande syrejoner från jordens jonosfär. Dessa joner strömmar under vissa förhållanden upp i magnetosfären. För att inte dessa joner ska falla tillbaka igen av gravitationen måste de accelereras ytterligare så att de når flykthastighet. De utflödande syrejonerna som studerats kommer från den del av jonosfären som svarar mot polarklyftan och som är en av de viktigaste källorna till syrejoner i magnetosfären. I polarklyftan och manteln är upphettning vinkelrätt mot jordens magnetiska fält vanligare än parallell acceleration genom ett fältparallellt elektriskt fält. Det är troligt att vinkelrät upphettning av joner är viktigt för jonutflöde och en av de troliga förklaringarna till vinkelrät upphettning är våg-partikelväxelverkan. I denna avhandling visas att upphettning genom våg-partikelväxelverkan som tidigare visats vara effektiv på lägre höjd, också kan vara effektiv på högre höjder. Den andel av vågaktiviteten som är effektiv i jonupphettningen måste vara nära 50 % på hög höjd, för att en cyklotronresonansmodell ska kunna förklara observerade temperaturer. Detta i kontrast till situationen på lägre höjd, där några få procent räcker. Vi har visat att det finns en tydlig koppling mellan temperaturen och vågintensiteten vid gyrofrekvensen vid varje mätpunkt. Vi har beskrivit medelvågintensiteten och den motsvarande hastighetsdiffusionskoefficienten som funktion av höjd på ett sätt som är användbart för modeller.

Vi har genom fallstudier visat att för de undersökta fallen är områdena med hög vågaktivitet och förhöjda jontemperaturer typiskt många jongyroradier stora i sin utbredning vinkelrätt mot magnetfältet. De observerade vågorna är sporadiska och spektraltätheten har en stor variation. Vi har även kunnat visa att större delen av vågaktiviteten på hög höjd har egenskaper som överensstämmer med Alfvénvågor och inte med statiska strukturer som driver förbi satelliten.

# List of included papers

The thesis is based on the following papers,

I Nilsson, H., Waara, M., Arvelius, S., Marghitu, O., Bouhram, M., Hobara, Y., Yamauchi, M., Lundin, R., Rème, H., Sauvaud, J.-A., Dandouras, I., Balogh, A., Kistler, L. M., Klecker, B., Carlson, C. W., Bavassano-Cattaneo, M. B., Korth, A. Characteristics of high altitude oxygen ion energization and outflow as observed by Cluster: a statistical study. *Annales Geophysicae, Volume 24, Issue 3, 2006, pp.1099-1112.*

II Waara, M., Nilsson, H., Stenberg, G., André, M., Gunell, H., Rème, H. Oxygen ion energization observed at high altitudes. *Annales Geophysicae, Volume 28, Issue 4, 2010, pp.907-916.*

III Waara, M., Slapak. R., Nilsson, H., Stenberg, G., André, M., Barghouthi, I.A. Statistical evidence for $O^+$ energization and outflow caused by wave-particle interaction in the high altitude cusp and mantle. *Annales Geophysicae, 2011. In revision.*

IV Slapak, R. and Nilsson, H. and Waara, M. and Stenberg, G. and André, M. $O^+$ heating associated with strong wave activity in the high altitude cusp and mantle. *Annales Geophysicae, 2011. In press.*

V Waara, M., Nilsson, H., Slapak. R., André, M., Stenberg, G. Statistical evidence for ion energization by waves in the high altitude cusp and mantle, *Geophys. Res. Lett., 2011. Submitted.*

# Other papers by the author

- Nilsson, H., Waara, M., Marghitu, O., Yamauchi, M., Lundin, R., Rème, H., Sauvaud, J.-A., Dandouras, I., Lucek, E., Kistler, L. M., Klecker, B., Carlson, C. W., Bavassano-Cattaneo, M. B., Korth, A. Transients in oxygen outflow above the polar cap as observed by the Cluster spacecraft. *Annales Geophysicae, Volume 26, Issue 11, 2008, pp.3365-3373.*

- Nilsson, H., Waara, M., Marghitu, O., Yamauchi, M., Lundin, R., Rme, H., Sauvaud, J.-A., Dandouras, I., Lucek, E., Kistler, L. M., Klecker, B., Carlson, C. W., Bavassano-Cattaneo, M. B., Korth, A. An assessment of the role of the centrifugal acceleration mechanism in high altitude polar cap oxygen ion outflow. *Annales Geophysicae, Volume 26, Issue 1, 2008, pp.145-157.*

- Lindstedt, T., Y. V. Khotyaintsev, A. Vaivads, M. André, H. Nilsson, and M. Waara , Oxygen ion energization by waves in the high altitude cusp and mantle, *Geophys. Res. Lett., 37, L09103, 2010.*

# Contents

# 1

# Introduction

Phenomena in the sky have fascinated mankind since the very beginning of our time here on Earth. The most varied and exciting sky on Earth is the one in the polar region, midnight sun in the summer and aurora during the darker period of the year. Aurora Borealis is a very beautiful example of the interaction between the solar wind and the magnetic field of the Earth. Along the open magnetic field lines in the polar cap (one end is connected to the Earth and the other to the solar wind) particles from the magnetosphere enter the Earth's atmosphere. The accelerated particles collide with and excite the atmospheric atoms and molecules, which then deexcite, emitting light.

The connection between the magnetic field lines of the polar cap and interplanetary space facilitates the escape of sufficiently energized ionospheric ions, both by allowing the transfer of energy from the solar wind and by providing an effective escape path from the magnetosphere and into the magnetosheath. The outflow from the polar cap regions along open magnetic field lines is the outflow most likely to lead to atmospheric loss.

Direct measurements (*in situ*) in space have provided knowledge about physical phenomena which cannot be registered at a distance. The measurements in situ have given us knowledge about processes, structures and characteristics in space plasma. The measurements made in space have changed our idea about the area close to the Earth as well as about outer space. Before the space age, our idea of outer space was simple. The magnetic field from the Earth was a dipole and was expected to be negligible at large distance from the Earth.

But even after the modern picture of the magnetosphere was established many important things were misunderstood. The common belief was that the plasma in the magnetosphere was consisted solely of hydrogen ions, i.e. the plasma around the Earth was hydrogen plasma, transported from the sun to the Earth by the solar wind. Now we know that a large part of the plasma is oxygen plasma coming up from the ionosphere of the Earth (Shelley et al., 1972). Energization and outflow of those oxygen ions caused by wave-particle interaction are the subject of this thesis.

# 2

# The near-Earth space environment

Plasma is an ionized gas, in which the atoms are dissociated into positive ions and negative electrons. It is often said that 99 % of the visible matter in the universe is in the plasma state (Chen, 1984). A charged particle in motion is a source of electric- and magnetic fields. These fields affect the motion of other charged particles far away and the plasma shows a collective behavior. One can usually assume that the plasma is quasineutral, i.e. neutral enough so that the electron density is approximately equal to the ion density ($n_e \simeq n_i$), but not necessarily so neutral that all the electromagnetic forces vanish.

The sun emits a high-speed stream of particles, the solar wind, which is composed of plasma. The solar wind affects and interacts with planets in our solar system. For magnetized planets such as Earth, the magnetosphere acts as a shield against the solar wind flow, forcing the solar wind plasma to be deflected around the shield. The solar wind plasma consists mainly of electrons and protons with a fractions of $He^{2+}$ ions. Since Earth is shielded by its magnetic field, only a tiny fraction of all the particles in the solar wind which impinge on the magnetospheric boundary will reach the Earth. The solar wind magnetic field is said to be frozen into the plasma, i.e. the magnetic field moves with the plasma. This means that if we follow a surface moving with the plasma flow, the magnetic flux through the surface will remain constant even as the surface changes its location and its shape (Kivelson and Russell, 1995). The interplanetary magnetic field (IMF) is the solar magnetic field carried away from the sun by the solar wind.

The Earth's magnetosphere is formed by the interaction between the solar wind and the internal dipole-like magnetic field of the Earth. The magnetosphere consists of various plasma regions. Fig. 2.1 shows what we today think that the surroundings of the Earth look like. The bow shock is the boundary where the supersonic solar wind slows down to subsonic speeds. The region behind the bow shock, where the plasma deflects around the Earth is the mag-
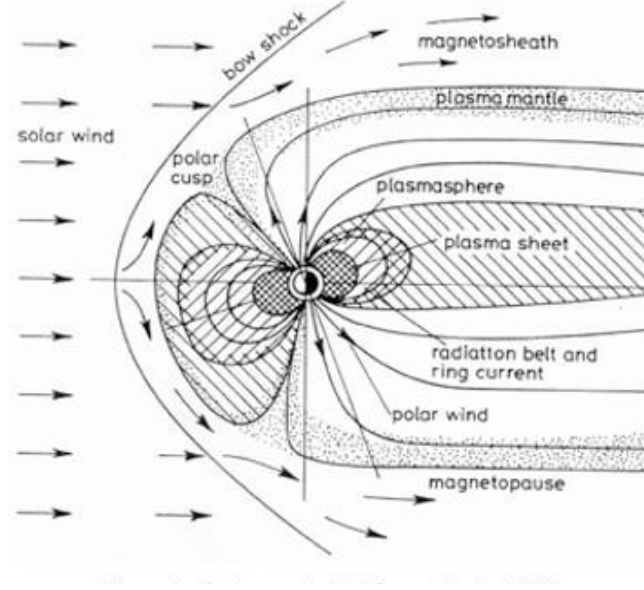
Figure 2.1: The Earth's magnetosphere and its different plasma regions. Source: Davies (1990).

netosheath. The magnetosheath is a turbulent region with shocked solar wind plasma (Kivelson and Russell, 1995).

The whole region with magnetic fields originating from the Earth is called the magnetosphere; the magnetopause is the outer border of the Earth's magnetospere just inside of the magnetosheath. The magnetopause boundary is located where the dynamic pressure of the streaming solar wind particles balances the magnetic pressure of Earth's magnetic field,

$$\rho_{sw} U_{sw}^2 = \frac{B_M^2}{2\mu_0} \tag{2.1}$$

where $\rho_{sw}$, $U_{sw}$ are the plasma mass density and the solar wind velocity, and $B_M$ is the magnetospheric magnetic field. The shape of the magnetosphere is compressed in the the sun-ward direction and it is extended in the anti-sunward direction. The magnetopause is located at about 10 Earth radii ($R_E$) in the sunward direction. When the solar wind is more intense, the magnetosphere shrinks and the magnetopause moves toward the Earth.

There is a funnel-shaped area between the sunward magnetic field and the tailward magnetic field, called the polar cusp. In the cusp, magnetosheath plasma can enter the magnetosphere along open field lines, i.e. field lines magnetically connected both to the Earth's ionosphere and the solar wind. The cusp position depends on changes in IMF orientation and solar wind pressure. The

converging magnetic field focuses the solar wind particles and allows study of a very large area of the magnetopause through a limited region of space inside the cusps. Tailward of the cusp is the mantle area. The mantle is populated by a mixture of magetosheath plasma and ionospheric plasma that has flown up from the cusp and polar cap. The upward flow from the polar cap is known as the polar wind. The different outflow regions are shown in Fig. 2.2.

The polar cap is the area around the geomagnetic pole bounded by the auroral oval (Kivelson and Russell, 1995). Polar caps are the high latitude regions in both hemispheres with open magnetic field lines connected to the interplanetary magnetic field, IMF. At high altitudes the field lines from the polar caps form the tail lobes in the magnetotail. The polar cap geometry varies considerably with the magnitude and orientation of the IMF.
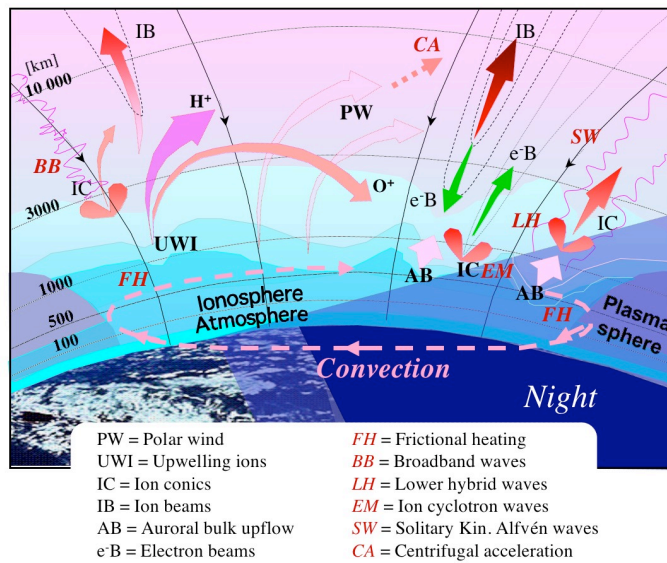


Figure 2.2: The outflow regions. Figure provided by R. Lundin.

The magnetic field of the Earth plays an important role in atmospheric escape. It keeps the potentially escaping ions confined within the Earth's magnetosphere. If ions flowing up from the polar cap are to escape they must not only overcome gravity, they must also be accelerated enough to leave the magnetosphere. Even if a particle is on an open field line when it starts its journey along a field line, the field line may close through magnetotail reconnection before the ion escapes into interplanetary space. In such a case, the magnetotail return flow will bring the ions back towards the Earth. The total loss rate of the atmosphere is around a few kilograms per second (Engwall, 2009).

In order to understand ion escape from a magnetized planet we must un-

derstand the initial ionospheric upflow and energization necessary to overcome gravity as well as the subsequent energization necessary to escape the magneto-sphere. We also need to understand the return flow in the tail and the eventual fate of these returning ions – loss to the atmosphere or to interplanetary space.

# 3

# Basic processes in space plasmas

The following chapter will briefly describe the basic features that determine the motion of a charged particle in magnetic and electric fields. More detailed descriptions can be found in various plasma and space physics textbooks, (see for example: Chen, 1984; Fälthammar, 1990; Parks, 1991; Kivelson and Russell, 1995).

## 3.1 Particle motion in a dipole field

By using the Lorentz equation, the equation of motion of a charged particle can be written as

$$m\frac{d\mathbf{v}}{dt} = q(\mathbf{E} + \mathbf{v} \times \mathbf{B}) \qquad (3.1)$$

where $m$ is the mass, $\mathbf{v}$ the velocity vector, $q$ the charge, $\mathbf{E}$ the electric field and $\mathbf{B}$ the magnetic field. The $\mathbf{v} \times \mathbf{B}$ force will cause a rotation around the magnetic field. The direction of rotation depends on the sign of the charge.

Viewing the particle motion in the direction of the magnetic field vector, negatively charged particles rotate clockwise and positively charged particles rotate anticlockwise. In both cases the particle's movement represents a current circling around the magnetic field anticlockwise and this gives a magnetic field opposite to the original. Consider a charged particle which moves in a homogeneous magnetic field in the absence of an electric field. Perpendicular to the magnetic field the particle has a circular orbit with a constant cyclotron angular frequency, $\omega_c$. The magnetic force $qv_\perp B$ and the centrifugal force $mv_\perp^2/r$ must be equal. The gyroradius (also called cyclotron or Larmor radius) of the particle is then obtained as

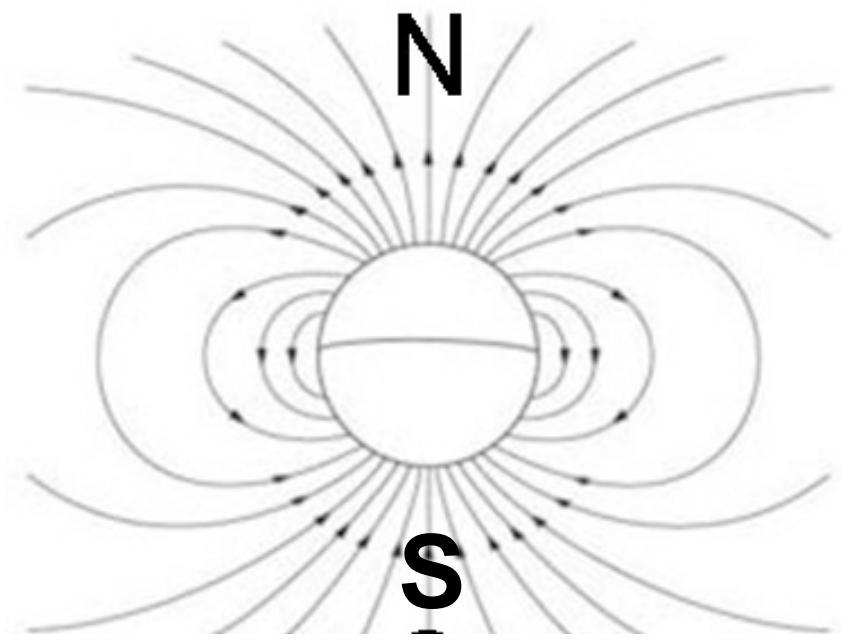$$r_L = \frac{mv_\perp}{|q|B} \qquad (3.2)$$

Figure 3.1: Sketch of a dipole magnetic field.

A particle that gyrates around a magnetic field line in a dipole magnetic field, (see Fig. 3.1), and has a velocity component along the magnetic field line, will move in a spiral motion with a magnetic moment,

$$\mu = \frac{mv_{\perp}^2}{2B} = \frac{mv^2}{2B} sin^2\alpha \qquad (3.3)$$

where $v$ is the total velocity and $\alpha$ is the pitch angle. The pitch-angle is the angle between the magnetic field $\mathbf{B}$ and the velocity vector of the particle $\mathbf{v}$. The pitch-angle $\alpha$ is defined by

$$\alpha = tan^{-1}\left(\frac{v_{\perp}}{v_{\parallel}}\right) \qquad (3.4)$$

When a particle is coming from a weak-field region into a strong-field region, $v_{\perp}$ must increase in order to keep $\mu$ constant. Since the total kinetic energy must remain constant due to the energy conservation, $v_{\parallel}$ must decrease when the magnetic field increases. If the magnetic field gradient is strong enough, an incoming particle ends up with a zero velocity along the magnetic field and the particle will be reflected back to the weak-field region. The point at which the reflection occurs is called the mirror point.

If there is an electric field perpendicular to the magnetic field then the particle drifts perpendicular both to the magnetic and the electric field. This perpendicular drift is given by

$$\mathbf{u}_\perp = \frac{\mathbf{E} \times \mathbf{B}}{B^2} \tag{3.5}$$

and is often referred to as an $E \times B$ drift. The $\mathbf{E} \times \mathbf{B}$ drift is independent of $q,m$ and $v_\perp$, i.e. ions and electrons will drift in the same direction and with the same velocity.

If there is an electric field parallel to the magnetic field the particles will be accelerated in the parallel direction. The acceleration depends on the sign of the charge and the electrons and protons are accelerated in opposite directions.

The above equations describe the fundamental particle movements that are important to us. In additional to those movements, it is worth mentioning a few other drifts.

For inhomogeneous magnetic fields, there will also be a gradient drift ($\nabla B$ drift). The gradient drift is given by

$$\mathbf{u_g} = \frac{1}{2} m v_\perp^2 \frac{\mathbf{B} \times \nabla \mathbf{B}}{qB^3} \tag{3.6}$$

and is dependent on $q,m$ and $v_\perp$, i.e. ions and electrons will drift in opposite directions. The curvature of the magnetic field will introduce an additional drift, the curvature drift

$$\mathbf{u_c} = \frac{m v_\parallel^2 \mathbf{R_c} \times \mathbf{B}}{qB^2 R_c^2} \tag{3.7}$$

where $R_c$ is the radius of curvature. Also the curvature drift is dependent of $q,m$ and $v_\perp$, i.e. ions and electrons will drift in opposite directions. The ring current inside the magnetosphere is produced by the motion of charged particles which undergo gradient and curvature drifts.

There is one more effect worth mentioning in the context of ion heating and outflow. It is a mechanism called centrifugal acceleration. It occurs for a changing magnetic field in the presence of a finite convection electric field. The centrifugal acceleration of charged particles moving along magnetic field lines in the presence of a finite convection electric field is

$$\frac{dv_\parallel}{dt} = \mathbf{u_g} \cdot \frac{d\hat{b}}{dt} = \mathbf{u_g} \cdot \left( \frac{\partial \hat{b}}{\partial t} + v_\parallel \frac{\partial \hat{b}}{\partial s} + (u_g \cdot \nabla)\hat{b} \right) \tag{3.8}$$

where $v_\parallel$ is the field-aligned (parallel) velocity of the particle, $u_g$ is the $E \times B$ drift, $s$ is a vector along the magnetic field direction and $\hat{b}$ is the unit vector in the direction of the magnetic field (Northrop, 1963; Cladis, 1986).

## 3.2   Waves in plasmas

In a collisionless plasma the particles are affected by electric and magnetic fields, not collisions. When the electrons in a plasma are displaced from a uniform background of ions, the charge displacement will result in electric fields, which

will restore the neutrality of the plasma by pulling the electrons back toward their original positions. Because of the inertia of the electrons, they will overshoot and oscillate around their equilibrium positions with a characteristic frequency known as the plasma frequency, $\omega_p$

$$\omega_p = \sqrt{\frac{n_0 e^2}{\epsilon_0 m}}. \tag{3.9}$$

The plasma frequency is the fundamental frequency in a plasma. It is a high frequency oscillation involving electron motion. There are many other wave modes involving both electrons and ions. Many of the wave modes involving ions are affected by the presence of a background magnetic field. For such waves the ion cyclotron frequency is another fundamental frequency. For heating of ions, lower frequency waves, which also involve the ions, which have more inertia and are moving slower than the electrons, are most important.

Both electrostatic waves and electromagnetic waves may propagate in a plasma. For electrostatic waves the electric field perturbation associated with the wave is parallel to the direction the wave vector, k, ($E \parallel k$) so that there are no magnetic perturbations associated with the wave. An electromagnetic wave, in contrast, must have a transverse component (perpendicular to k), but may also have a component parallel to k.

Ordinary light waves are transverse electromagnetic waves in which the wave vector, $\mathbf{k}$, is perpendicular to both the electric field and the magnetic field of the wave. The angular frequency for ordinary light waves is given by $\omega = ck$, where $c$ is the speed of light. In a plasma the angular wave frequency, $\omega$, is generally a more complicated function of $\mathbf{k}$. Plasma waves depend on the angle between its direction of propagation and the external magnetic field, and the angular frequency is a function of both $k_\perp$ and $k_\parallel$. If the frequency is plotted versus $k_\perp$ and $k_\parallel$, which are the components of the wave vector perpendicular and parallel to the external magnetic field, we obtain so-called dispersion surfaces. André (1985) shows how such dispersion surfaces constitute an elegant way of viewing plasma waves. Each point on the surface represents a wave at a certain frequency, with a certain wavelength and propagation direction, and the entire surface may be referred to as a wave mode. Interested readers are urged to consult that paper for more details.

André et al. (1998) investigated how ion heating is associated with broadband low-frequency wave fields (BB-ELF), waves near the lower hybrid (LH) frequency, and electromagnetic ion cyclotron (EMIC) waves near half the proton gyrofrequency.

Broadband waves are often observed in association with transverse ion energization. At lower (up to 5 $R_E$) altitude these waves are found to be one of the most important sources of energization of the ionospheric outflow (André et al., 1998; Norqvist et al., 1998). Only a fraction of the observed wave activity in the broadband waves appeared to be efficient in heating the ions. Broadband waves observed with the Freja spacecraft were consistent with Alfvén waves at frequencies up to a few Hz (André et al., 1998)). As at lower altitudes, the

observed broadband waves can explain the observed $O^+$ energies measured in the high altitude cusp/mantle region. The broadband waves we have observed in the high altitude (5-15 $R_E$) region, and report in this thesis, are consistent with left-hand polarized Alfvén waves. The Alfvén wave propagates with the Alfvén velocity, $v_a$

$$v_a = \frac{B_0}{\sqrt{\mu_0 m_i n_i}} \qquad (3.10)$$

which can be calculated from measured plasma parameters (ion mass density) and the measured background magnetic field.

# 4

# Ion energization

The ionospheric projection of the cusp/polar cap is an important source of outflowing oxygen ions. Ionospheric plasma may flow up from the ionosphere but at velocities, which are low enough that the ions are still gravitationally bound (Nilsson et al., 1996). For the ions to overcome gravity, further acceleration is needed. The main energization mechanisms that are known for ionospheric $O^+$ are ambipolar diffusion, wave-particle interaction, parallel potential drops and centrifugal acceleration (see André and Yau, 1997; Yau and André, 1997; Lotko, 2007). The energization needed for the particles to escape from the magnetosphere is even larger (see discussion in Seki et al., 2001). This chapter discusses energization perpendicular to the magnetic field by wave-particle interaction.

## 4.1   Observation of ion heating at high altitude

In the cusp/polar cap, transverse heating is more common than field-aligned acceleration through a magnetic field-aligned electric field. It is thus believed that transverse heating of ions is important for ion outflow and one of the probable explanations for transverse heating is wave-particle interaction (Moore and Horwitz, 2007).

One type of efficient ion energization is caused by left-hand polarized waves, with wavelengths much larger than the ion gyroradius and at frequencies near the ion gyrofrequency. The E-field vector of the wave rotates in the same direction as ions around the magnetic fields and energizes the ions by resonant heating. This ion cyclotron resonance mechanism can be investigated using test-particle calculations or Monte-Carlo simulations (Retterer et al., 1987; Chang et al., 1986).

Many studies (see Chang et al., 1986; Barghouthi et al., 1998; Barghouthi, 2008; Bouhram et al., 2003, 2004, and references therein) have investigated the effect of wave-particle interaction on the ion outflow. Wave-particle interaction can be described by a quasi-linear velocity diffusion rate in ion velocity space, caused by waves around the ion gyrofrequency (Retterer et al., 1987; Chang

et al., 1986). Studies at lower altitudes (up to 5 $R_E$: see Norqvist et al., 1996; André et al., 1998; Bouhram et al., 2003) found that only one to ten of percent of the observed electric field spectral density around the oxygen gyrofrequency needs to be in resonance with the ions to obtain the measured $O^+$ energies.

Bouhram et al. (2004) investigated the altitude dependence of transversely heated $O^+$ distributions in the cusp region up to 6.5 Earth radii ($R_E$). Nilsson et al. (2006) showed that the high altitude polar cap magnetosphere (5 – 15 $R_E$) is not just a passive transport region, and that a significant perpendicular energization at high altitudes was a likely explanation for the reported measurements. They found that there is significant transverse energization of $O^+$ in the high altitude region (5 – 15 $R_E$), indicated both by perpendicular temperatures increasing with altitude as well as by a tendency towards higher perpendicular than parallel temperature for the highest observed temperatures. Arvelius et al. (2005) demonstrated that the statistical distribution of energetic ions (1 keV and above) in the 6 – 12 $R_E$ geocentric distance interval was not consistent with just a low altitude heating source, there was clear evidence for heating occurring also at higher altitude. In the work presented in this thesis we have extended the studies by Nilsson et al. (2006); Arvelius et al. (2005), investigating the processes behind the ion heating observed at high altitude.

## 4.2    Modelling of ion heating and outflow

We have investigated ion heating by using a test particle model based on the theory described by **?**). The theory used in the test-particle model described by Chang et al. (1986) is the same theory as in Retterer et al. (1987), but Chang used a test-particle simulation and Retterer used the velocity diffusion coefficient in a Monte Carlo simulation.

The calculation of the net increase of the perpendicular energy of the ions in the test-particle calculation is based on mean values over many gyroperiods. The heating rate is given by

$$\frac{dW}{dt} = S_L \frac{q^2}{2m} \tag{4.1}$$

where $q$ and $m$ are the charge and the mass of the ion and $S_L$ is the power spectral density of the electric field at the $O^+$ gyrofrequency due to left-hand polarized waves. As the ions move up along the field lines, they interact with waves at a frequency that is in local resonance with them. The heating continues as long as the wave intensity remains strong.

The electric field is measured by the EFW instrument in the spacecraft reference frame, with unknown Doppler shift. For the broadband waves observed in our studies we have assumed that we do not have significant Doppler shift of the waves. We could show in paper III that the observed electric and magnetic fields were not consistent with electrostatic structures drifting past the spacecraft, while they were consistent with Alfvén waves. For the case study

in paper II a hodogram reveals that the waves are left-hand polarized. For statistical studies, it is not feasible to make a hodogram for all the measurement points. In the statistical studies presented in paper III and V we have assumed 50 % of the wave activity to be due to left-hand polarized waves.

Chang et al. (1986) also provided an asymptotic solution yielding both perpendicular and parallel temperature from the locally observed waves and the shape of the electric field frequency spectrum. In practice, locally observed waves mapped along the magnetic field lines are used. The spectral density, S, as a function of frequency, f, can often be approximated by $S(f) \propto f^{-\alpha}$, with $\alpha$ as a power law fitting parameter, and the gyrofrequency can often be assumed to fall off with the cube of the geocentric distance, $f_i(r) \propto r^{-3}$, allowing mapping to an arbitrary altitude. The mean energy ratio $W_\perp/W_\parallel$ asymptotically approaches a constant value of $(6\alpha + 2)/9$. In this limit, the total ion energy is insensitive to the choice of initial conditions, making it suitable for a comparison with our data. The result for the total ion energy, $W = W_\parallel + W_\perp$ (Retterer et al., 1987), is

$$W = \left(3\alpha + \frac{11}{2}\right)^{1/3} m \left[\frac{rD_\perp(r)}{(3\alpha + 1)}\right]^{2/3} \tag{4.2}$$

where the quasi-linear velocity diffusion rate perpendicular to the geomagnetic field is given by

$$D_\perp = \frac{\eta q^2}{4m^2} \mid E_x(\omega = \Omega) \mid^2 \tag{4.3}$$

where $q$ is the charge, $\Omega$ is the ion gyrofrequency, $\omega$ is the wave frequency, $|E_x|^2$ is the electric field spectral density at the local ion gyrofrequency and $\eta$ is the proportion of the measured spectral density that corresponds to a left-hand polarized wave.

The parallel and perpendicular components can be derived from the total ion energy and the ratio between the perpendicular and parallel energy (Barghouthi, 1997)

$$W_\parallel = \frac{9m}{2^{1/3}} \left[\frac{rD_\perp(r)}{(3\alpha + 1)(6\alpha + 11)}\right]^{2/3} \tag{4.4}$$

$$W_\perp = \frac{(6\alpha + 2)m}{2^{1/3}} \left[\frac{rD_\perp(r)}{(3\alpha + 1)(6\alpha + 11)}\right]^{2/3}. \tag{4.5}$$

A more advanced Monte Carlo model is described in Barghouthi et al. (2007). The effect of altitude and velocity dependent wave-particle interactions on $O^+$ and $H^+$ ion outflows was studied for conditions representative of the auroral region using a Monte Carlo simulation. A further step is to also follow the plasma as it is moving with the magnetospheric convection, as has for example been done by Zeng et al. (2006).

The Earth's magnetic field is a dipole, but the solar wind perturbs the dipole field. Close to the magnetopause, and in particular in the magnetotail, the shape of the magnetic field is not dipole-like. It is usually assumed that a dipole model is a decent approximation out to about 10 $R_E$ distance. The average measured

background magnetic field presented in Fig. 4.1 shows that a dipole model for the average magnetic field up to 12 $R_E$ is a good approximation but at even higher altitudes the decrease of the measured background magnetic field with altitude is smaller than for a dipole field for our data set. Many of our measurements are from higher altitude than 12 $R_E$ and we have chosen to use the average measured magnetic field values rather than the dipole model in test-particle calculations made in the paper III, IV and V.
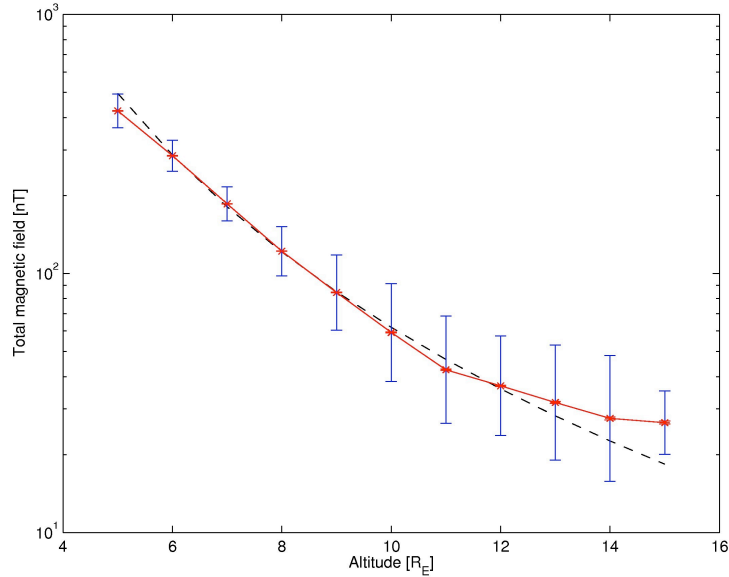


Figure 4.1: Profile of the total magnetic field versus altitude in the high altitude cusp and mantle region. The blue error bars show the standard deviation for the logarithmic values. The black dashed line is the dipole model.

As transversely heated ions move outward, their transverse energy is gradually converted to parallel energy by the mirror force. Such transversely heated and subsequently outflowing ions are known as *conics* due to their shape in velocity space (see André and Yau, 1997; Yau and André, 1997; Moore et al., 1999). If a heated population leaves the heating region and drifts adiabatically along the field lines the mirror force will transfer perpendicular energy into parallel energy; the further away from the heating region the ions are observed, the more parallel energy they have. The relatively sporadic appearance of enhanced wave activity presented in Waara et al. (2010) may make it difficult to observe the actual heating. The heating from the waves can occur for just a few minutes but the total energy gains for the particles remain, and the increased perpendicular temperature remains for some time after the actual heating has

stopped. It is therefore important to assess how the ion distributions evolve once they leave a heating region. For how long will they retain a high perpendicular temperature in the absence of heating?
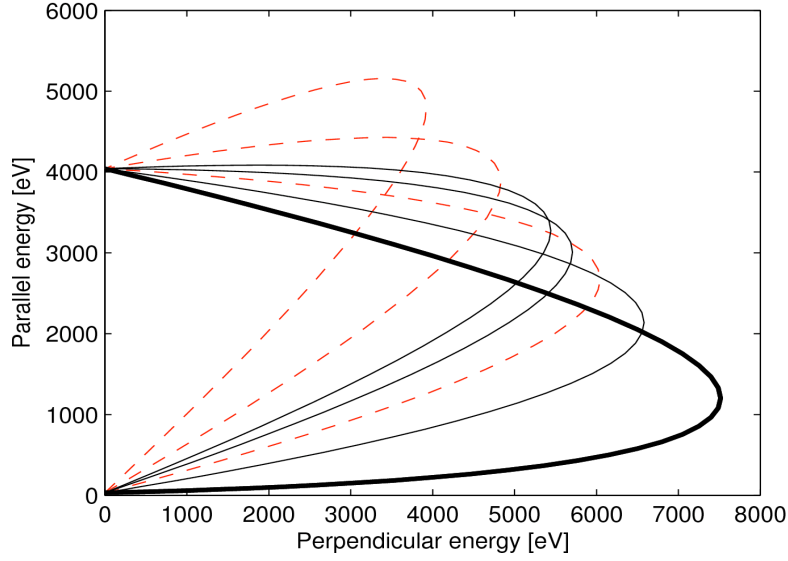


Figure 4.2: The folding of perpendicularly heated particles starting at 12 $R_E$. The thick black line represents the initial velocity space contour at 12 $R_E$. The three different curves in the same color (red dashed and thin black) corresponds to the three different altitudes (13, 14 and 15 $R_E$). The values for a dipole magnetic field are represented by the red dashed lines. The thin black lines represent the values for the measured background magnetic field.

In Fig. 4.2 we investigate the folding of one contour line in the velocity space of a perpendicularly heated particle population starting at 12 $R_E$ and ending at 15 $R_E$. The initial velocity space contour used in the simulation is shown in Fig. 4.2 using a thick black line. The particles are moving outward along the field line without any heating. The three different curves in the same color corresponds to the different altitudes (13, 14 and 15 $R_E$). The thin black lines show the result for ions moving in the measured background magnetic field and the red dashed lines show the case of a dipole magnetic field. The decrease of the perpendicular temperature is around 10 % for each $R_E$ if the measured background magnetic field is used and is around 20 % for each $R_E$ if the dipole model is used. Fig. 4.2 clearly shows that a perpendicularly heated population remains perpendicularly heated also after the distribution has traveled along the magnetic field lines for a few $R_E$. The high perpendicular temperatures

measured at high altitudes may result from heating at lower altitude or at lower latitude. The results show that strongly heated ions are likely to be observed with an enhanced perpendicular temperature over rather large regions outside the actual heating region. This result is used in paper V, but the figure was not presented due to the page limit of *Geophysical Research Letters*.
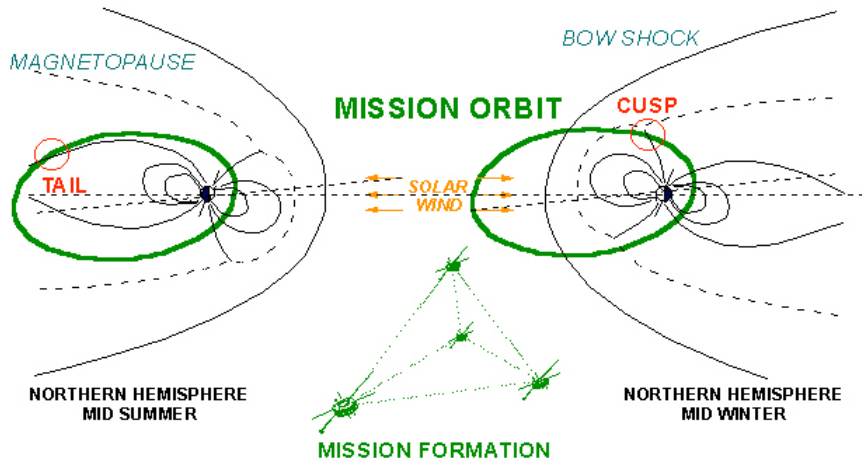
# 5

# The Cluster mission



Figure 5.1: Cluster spacecraft seasonal orbits. The winter orbits correspond to high altitude passes over the polar cap. (The figure is adopted from European Space Agency, 2000)

## 5.1 Mission description

The Cluster mission consists of four spacecraft and was launched by ESA in 2000. The mission was declared operational on 1 February 2001 (Escoubet et al., 2001). The main goal of the Cluster mission is to study small-scale plasma structures in three dimensions in the key plasma regions, such as the magnetotail, the polar cusps, the auroral zones, the magnetopause, the solar wind and the bow shock. The separation distances between the spacecraft have varied between 100 km and 20 000 km, to address the relevant spatial scales.

This constellation allows one to do three-dimensional mapping of space and to distinguish between temporal and spatial structures. The Cluster spacecraft has an elliptical polar orbit, with a perigee altitude of 19 000 km ($\approx 3\ R_E$) and an apogee altitude of 119 000km ($\approx 19\ R_E$). The spacecraft are spin-stabilized with a spin period of about 4 s, while the orbital period is 57 hours. The orbit varies with the season according to Fig. 5.1 (European Space Agency, 2000).

## 5.2   Instrument description

Each Cluster satellite carries the same set of eleven instruments to investigate charged particles, electric fields and magnetic fields. Table 5.1 shows a summary of the instruments on Cluster.

| Acronym | Instrument |
|---|---|
| FGM | Fluxgate Magnetometer |
| STAFF | Spatio-Temporal Analysis of Field Fluctuation experiment |
| EFW | Electric Field and Wave experiment |
| WHISPER | Wave of High frequency and Sounder for Probing of Electron density by Relaxation |
| WBD | Wide Band Data |
| DWP | Digital Wave Processing experiment |
| EDI | Electron Drift Instrument |
| ASPOC | Active Spacecraft Potential Control |
| CIS | Cluster Ion Spectrometer |
| PEACE | Plasma Electron And Current Experiment |
| RAPID | Research with Adaptive Particle Imaging Detectors |
| WEC | Wave Experiment Consortium (STAFF, EFW, WHISPER, WBD and DWP) |

Table 5.1: Summary of the instruments on Cluster.

The data used in this study are spring data (January to May) from the years 2001 to 2003. This corresponds to high altitude passes over the polar cap. Most of the data were observed at altitudes between 5 and 15 $R_E$. The CIS, EFW and FGM instruments are used in this thesis and are briefly introduced here.

Three-dimensional ion distributions are measured with the Cluster Ion Spectrometer (CIS). The CIS instruments is described in detail in Rème et al. (2001). CIS consists of two different ion spectrometers, Composition Distribution Function (CODIF) which can resolve the major magnetospheric ions and Hot Ion Analyzer (HIA) which has no mass resolution but higher angular and energy resolution. We will only present results from the CODIF instrument. CODIF can resolve $H^+$, $He^+$, $He^{2+}$ and $O^+$ through a time-of-flight technique. The detector has a field-of-view of 360° orthogonal to the spin plane, divided into 16 sectors of 22.5° each. The angular resolution is likewise 22.5° in the spin plane.

The energy coverage in the modes of interest to us is from 15 eV per charge up to 38 keV per charge in up to 30 logarithmically spaced steps with a $\Delta E/E$ of 0.16.

The electric field and wave experiment (EFW) is designed to measure the electric field. EFW records two orthogonal electric field components in the satellite spin plane. In the normal mode data which we have used the sampling rate is 25 samples/second (Gustafsson et al., 2001).

The Cluster fluxgate magnetometer (FGM) measures the three-dimensional magnetic field vector. In our data set the sampling rate is 22.4 samples/second (Balogh et al., 2001).

## 5.3 Cross-talk in the CIS CODIF instrument
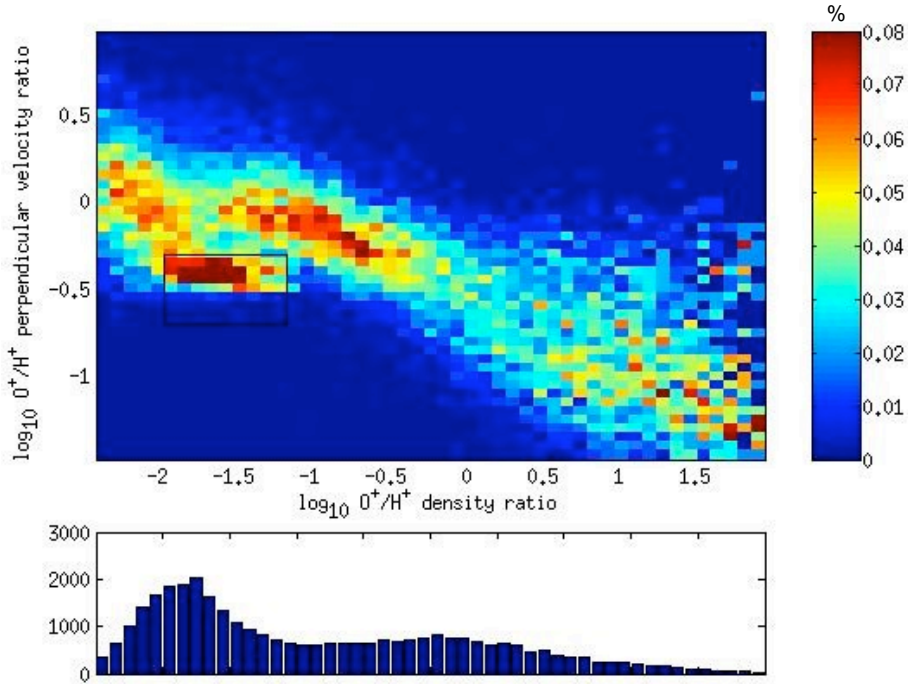


Figure 5.2: Upper panel: Distribution of $O^+/H^+$ perpendicular velocity ratio for each interval of $O^+/H^+$ density ratio. Each column is normalized: the sum of all data bins in a column is 100%. Lower panel: the number of data points contributing to each column.

The CODIF instrument is in principle very good at separating different masses (or more specifically mass per charge). In spite of this, for intense fluxes of $H^+$ other mass channels may be affected by false counts, a phenomenon known

as cross-talk. This is due to chance start-stop coincidences caused by high proton count rates. For intense enough fluxes of $H^+$ these chance coincidences will produce significant background counts also in the $O^+$ time-of-flight range. This can be checked *a posteriori* most of the time, because a data product containing the time-of-flight histogram (product 28, see Rème et al. (2001)) is often transmitted to ground for at least one spacecraft at a time. One may then check if the $O^+$ counts correspond to a local maximum at the corresponding times in the time-of-flight histogram. We have done this for a number of cases, but it is not feasible to use this technique in a statistical study. Instead we have utilized the fact that the $\boldsymbol{E} \times \boldsymbol{B}$ drift should dominate perpendicular drift and be the same for all ion species in the energy range and location studied (below 40 keV in the polar cap). For the case when the $O^+$ counts are all false counts caused by the intense $H^+$ fluxes seen simultaneously, the estimate of the $O^+$ $\boldsymbol{E} \times \boldsymbol{B}$ drift will be 1/4 of the estimate of the $H^+$ $\boldsymbol{E} \times \boldsymbol{B}$ drift. This is because the false $O^+$ counts appear in the same energy channels as the real $H^+$ counts (though at much lower intensity). When these counts are interpreted as $O^+$ all velocity moments are 1/4 of the corresponding $H^+$ velocity moments (the difference in velocity for the same energy being the square root of the mass ratio which is 16). The data set shows a clear peak in the distribution of $O^+$ vs. $H^+$ perpendicular drift at the one-to-four ratio (the peak is indicated with a black square in Fig. 5.2). Because of limited angular and energy resolution and random noise one cannot demand that the $O^+$ to $H^+$ perpendicular velocity ratio should be close to unity for uncontaminated data; there will be considerable scatter. Furthermore we want to keep $O^+$ obtained when there is no significant amount of $H^+$, in which case the relationship between $H^+$ and $O^+$ will be random. The important point is rather that for pure cross-talk the relation is not random, the velocity ratio is close to 4 and the density / flux ratio should be in a limited interval as well. Empirical tests, where we compare our criterion with visual inspection of spectrograms and time-of-flight data, indicate that demanding the velocity ratio to be between 0.2 – 0.5 and the density ratio below to 0.063 to identify cross-talk gives an interval which includes most of the cross-talk values without removing too much data which is not affected by cross-talk.

$H^+$ contaminated data is removed from the particle data set in all the papers included in this thesis.

# 6

# Future works

We have quantified transverse ion heating and the wave activity that leads to ion heating in our previous work. A possible next step is to investigate what drives the waves that cause the ion heating, and determine empirically under what conditions most wave activity is generated. We have a preliminary result that shows that strong wave activity is correlated with strong solar wind origin proton fluxes. The next step is to study ion and electron distribution functions in more detail, and to use the WHAMP code (Waves in Homogeneous Anisotropic Multi-component Plasmas, Rönnmark (1982)) to see if the proton distributions we observe are likely to generate significant cyclotron waves.

Another promising path would be to extend our previous Cluster work to cover a larger part of the solar cycle (extended from 2001-2003 to also include the low solar activity years of 2004 and 2005), and to include all Cluster orbits, not just the polar cap part. That way we can also study the mid-altitude cusp and the tail. The tail data can be used to study the role of magnetotail return flow in reducing net ion escape rates.

By compiling a list of extreme solar wind events and studying them separately we can extend the parameter range for which we have reliable empirical estimates of the ion escape.

# 7

# Summary of included papers

A general conclusion from our work on high altitude oxygen ion energization is that ion energization and outflow occur in the high altitude cusp and mantle. The particle are often heated perpendicularly to the geomagnetic field and resonant heating at the gyrofrequency is most of the time intense enough to explain the observed $O^+$ energies measured in the high altitude ($8 - 15$ $R_E$) cusp/mantle region of the terrestrial magnetosphere. The observed average waves can explain the observed average $O^+$ energies. We have also shown a clear correlation between temperature and wave intensity at the gyrofrequency at each measurement point. We have described the average wave intensity and corresponding velocity diffusion coefficients as a function of altitude in a format convenient for modelers. We have shown how large the variability of the observed electric fields is, and how sporadic the appearance of increased wave activity typically is. Based on three cases we have found that the regions with enhanced wave activity and increased ion temperature are typically many ion gyro radii in perpendicular extent.

Furthermore we have shown that the wave activity observed in this high altitude region is consistent with Alfvén waves, and inconsistent with static structures drifting past the spacecraft.

## Paper I: Characteristics of high altitude oxygen ion energization and outflow as observed by Cluster: a statistical study.

In the first paper we have made a statistical study of oxygen ion outflow using Cluster data obtained at high altitude above the polar cap. Moment data for both hydrogen ions ($H^+$) and oxygen ions ($O^+$) from 3 years (2001-2003) of spring orbits (January to May) have been used. The altitudes covered were mainly in the range 5–15 $R_E$. It was found that there is significant transverse

energization of $O^+$ at high altitudes, indicated both by high perpendicular temperatures for low magnetic field values as well as by a tendency towards higher perpendicular than parallel temperature distributions for the highest observed temperatures. We also found that the parallel bulk velocity is close to the same for a wide range of relative abundance of the two ion species, including when the $O^+$ ions dominate.

## Paper II: Oxygen ion energization observed at high altitudes.

In the second paper we present a case study of significant heating (up to 8 keV) perpendicular to the geomagnetic field of outflowing oxygen ions at high altitude ($12 R_E$) above the polar cap. The shape of the distribution functions indicate that most of the heating occurs locally (within $0.2 - 0.4 R_E$ in altitude). In contrast to many reported events observed at lower altitudes, it is not likely that the locally observed wave fields can cause the observed ion energization. Also, it is not likely that the ions have drifted from some nearby energization region to the point of observation. This suggests that additional fundamentally different ion energization mechanisms are present at high altitudes. One possibility is that the magnetic moment of the ions is not conserved, resulting in slower outflow velocities and longer time for ion energization. In light of our later studies, this case seems to be an exception. Most of the heating probably occurred just outside our observation region, even though judging from this initial data we found that unlikely.

## Paper III: Statistical evidence for $O^+$ energization and outflow caused by wave-particle interaction in the high altitude cusp and mantle.

The third paper contains a statistical study of the low ($< 1$ Hz) frequency electric and magnetic field spectral densities observed by the Cluster spacecraft in the high altitude cusp and mantle region. In the paper we have characterized statistically the distribution of low frequency electric and magnetic field spectral densities in the high altitude (5–15 $R_E$) cusp/mantle. The observed average waves can explain the average $O^+$ energies measured in the high altitude (8-15 $R_E$) cusp/mantle region of the terrestrial magnetosphere according to our test-particle calculations. The relation between the electric and magnetic field spectral densities results in a large span of phase velocities, from a few hundred km/s up to a few thousand km/s. In spite of the large span of phase velocities, the ratio between the calculated local Alfvén velocity and the estimated phase velocity is close to unity. This paper provide average values of a coefficient describing diffusion in ion velocity space at different altitudes. This coefficient can be used in studies of ion energization and outflow.

## Paper IV: O$^+$ heating associated with strong wave activity in the high altitude cusp and mantle.

In the fourth paper we use the Cluster spacecraft to study three events with intense waves and energetic oxygen ions (O$^+$) in the high altitude cusp and mantle. The ion energies considered are of the order 1000 eV and higher, observed above an altitude of 8 R$_E$ together with intense wave activity at the O$^+$ gyrofrequency. We show that heating by waves can explain the observed high perpendicular energy of O$^+$ ions, using a simple gyroresonance model and 25-45% of the observed wave spectral density at the gyrofrequency. This is in contrast to our previous study where the wave intensity was too low to explain the observed high altitude ion energies. Long lasting cases (>10 min) of high perpendicular-to-parallel temperature ratios are sometimes associated with low wave activity, suggesting that a high perpendicular-to-parallel temperature ratio is not a good indicator of local heating. Using multiple spacecraft, we show that the regions of enhanced wave activity are at least one order of magnitude larger than the gyroradius of the heated ions.

## Paper V: Oxygen ion energization by waves in the high altitude cusp and mantle

In the last paper we present a comparative study of low frequency electric field spectral densities and temperatures observed by the Cluster spacecraft in the high altitude cusp/mantle region. There is a clear correlation between O$^+$ temperature and wave intensity at the oxygen gyrofrequency at each measurement point. This correlation agrees with the predictions by both an asymptotic mean-particle theory and a test-particle approach. The perpendicular-to-parallel temperature ratio is also consistent with the predictions of the asymptotic mean-particle theory. The correlation is not perfect, and is not expected to be. At times the perpendicular temperature is significantly higher than predicted by the models and the simultaneously observed wave activity. Similarly there is a significant amount of data points where the temperature is higher than predicted by the models and the observed spectral density. Both are expected effects of sporadic heating. The models assume that the ions have experienced the same wave activity throughout their flight along the field line. If heating has ceased at the time of observation we observe cases with low wave activity as compared to observed temperatures. If heating has just started at the time of observation, observed temperatures will be lower than predicted by the models and observed wave activity. We observed waves of sufficient amplitude to explain the highest temperatures observed.

# Acknowledgments

First of all, I would like to thank my supervisor Hans Nilsson, who introduced me to space physics during my diploma work in 2004. Since then he has been a very good teacher, has patiently tryed to answer all my questions although I have asked some of the questions over and over again. Together we have struggled through ups and downs towards the goal, my PhD degree. Without your help this thesis would not have existed. Many, many thanks!

I would also want to thank the co-authors of my papers for fruitful collaborations. I would especially like to thank Professor Mats André and Gabriella Stenberg for the time they have spent on helping me with my papers.

This research work has been financed by the Swedish National Graduate School of Space Technology and the Swedish Institute of Space Physics (Institutet för rymdfysik, IRF). It has been a pleasure and a great experience to have had the possibility to do research in space physics.

I also wish to thank my neighbors on the fourth floor: Csilla Szasz, Johan Kero, Daria Mikhaylova, Ella Carlsson, Andreas Ekenbäck, Alla Belova, Maria Smirnova, Alexander Grigoriev, Katarina Axelsson, Rikard Slapak, Shahab Fatemi, Maria Mihalikova and Catherine Dieval. Jonas Ekeberg deserves a special thanks for the many hours we have spent sharing ups and downs and for helping me finish this thesis. Also Tony Giang deserves a special thanks for all the help and the good advice I have got from you. You have been a great support during the work with my thesis. I hope to see you all again!

Rick McGregor did a very careful proof-reading of my English which improved the readability and correctness throughout this thesis.

Also the rest of the staff at IRF deserve my gratitude for all their help and for creating a nice and friendly working environment during these years.

I would like to thank my parents and sisters for always showing an interest in what I am doing and for all their help. You have been a great support although never given the deserved gratitude.

Kajsa, the most important person, you are a fantastic mother and life partner. This thesis would not have been done without your support. Gustav, your appearance in our family made it a perfect moment to finish this thesis.

# Bibliography

André, M.: Dispersion surfaces, Journal of Plasma Physics, 33, 1–19, doi: 10.1017/S0022377800002270, 1985.

André, M. and Yau, A. W.: Theories and observations of ion energization and outflow in the high latitude magnetosphere, Space Sci. Rev., 80, $27 - 48$, 1997.

André, M., Norqvist, P., Andersson, L., Eliasson, L., Eriksson, A. I., Blomberg, L., Erlandson, R. E., and Waldemark, J.: Ion energization mechanisms at 1700 km in the auroral region, J. Geophys. Res., 103, 4199–4222, doi: 10.1029/97JA00855, 1998.

Arvelius, S., Yamauchi, M., Nilsson, H., Lundin, R., Hobara, Y., Rème, H., Bavassano-Cattaneo, M. B., Paschmann, G., Korth, A., Kistler, L., and Parks, G. K.: Statistics of high-altitude and high-latitude $O^+$ ion outflows observed by Cluster/CIS, Ann. Geophys., 23, $1909 - 1916$, 2005.

Balogh, A., Carr, C. M., Acuna, M. H., Dunlop, M. W., Beek, T. J., Brown, P., Fornaon, K.-H., Georgescu, E., Glassmeier, K.-H., Harris, J., Musmann, G., Oddy, T., and Schwingenschuh, K.: The Cluster Magnetic Field Investigation: overview of in-flight performance and initial results, Ann. Geophys., 19, $1207 - 1217$, 2001.

Barghouthi, I. A.: Effects of wave-particle interactions on $H^+$ and $O^+$ outflow at high latitude: A comparative study, J. Geophys. Res., 102, $22\,065$–$22\,076$, doi:10.1029/96JA03293, 1997.

Barghouthi, I. A.: A Monte Carlo study for ion outflows at high altitude and high latitude: Barghouthi model, Journal of Geophysical Research (Space Physics), 113, 8209, doi:10.1029/2008JA013274, 2008.

Barghouthi, I. A., Barakat, A. R., and Persoon, A. M.: The Effects of Altitude-Dependent Wave Particle Interactions on the Polar Wind Plasma, Astrophysics and Space Science, 259, 117–140, doi:10.1023/A:1001569207346, 1998.

Barghouthi, I. A., Doudin, N. M., Saleh, A. A., and Pierrard, V.: High-altitude and high-latitude $O^+$ and $H^+$ outflows: the effect of finite electromagnetic turbulence wavelength, Annales Geophysicae, 25, 2195–2202, doi: 10.5194/angeo-25-2195-2007, 2007.

Bouhram, M., Malingre, M., Jasperse, J. R., Dubouloz, N., and Sauvaud, J.-A.: Modelling transverse heating and outflow of ionospheric ions from the dayside cusp/cleft. 2 Applications, Ann. Geophys., 21(8), 1773–1791, 2003.

Bouhram, M., Klecker, B., Miyake, W., Rème, H., Sauvaud, J.-A., Malingre, M., Kistler, L., and Blăgău, A.: On the altitude dependence of transversely heated $O^+$ distributions in the cusp/cleft, Ann. Geophys., 22, $1787-1798$, 2004.

Chang, T., Crew, G. B., Hershkowitz, N., Jasperse, J. R., Retterer, J. M., and Winningham, J. D.: Transverse acceleration of oxygen ions by electromagnetic ion cyclotron resonance with broad band left-hand polarized waves, Geophys. Res. Lett., 13, 636–639, doi:10.1029/GL013i007p00636, 1986.

Chen, F. F.: Introduction to plasma physics and controlled fusion, Plenum Press, New York, second edn., 1984.

Cladis, J. B.: Parallel acceleration and transport of ions from polar ionosphere to plasmasheet, Geophys. Res. Lett., 13, $893-896$, 1986.

Davies, K.: Ionospheric Radio, Short Run Press Ltd., England, 1990.

Engwall, E.: Low-Energy Ion Escape from the Terrestrial Polar Regions, Ph.D. thesis, Uppsala University, Department of Physics and Astronomy, 2009.

Escoubet, C. P., Fehringer, M., and Goldstein, M.: The Cluster mission, Annales Geophysicae, 19, 1197–1200, 2001.

European Space Agency: Cluster seasonal orbits, http://sci.esa.int/science-e/www/object/index.cfm?fobjectid=24451, 2000.

Fälthammar, C.: Rymdfysik, Institutionen för Plasmafysik, Kungliga Tekniska Högskolan, second edn., 1990.

Gustafsson, G., André, M., Carozzi, T., Eriksson, A. I., Fälthammar, C.-G., Grard, R., Holmgren, G., Holtet, J. A., Ivchenko, N., Karlsson, T., Khotyaintsev, Y., Klimov, S., Laakso, H., Lindqvist, P.-A., Lybekk, B., Marklund, G., Mozer, F., Mursula, K., Pedersen, A., Popielawska, B., Savin, S., Stasiewicz, K., Tanskanen, P., Vaivads, A., and Wahlund, J.-E.: First results of electric field and density observations by Cluster EFW based on initial months of operation, Annales Geophysicae, 19, 1219–1240, 2001.

Kivelson, M. and Russell, C.: Introduction to Space physics, Cambridge University press, 1995.

Lotko, W.: The magnetosphere-ionospher system from the perspective of plasma circulation: A tutorial, J.Atmos.Solar-Ter.Phys, 69, 191–211, doi: 10.1016/j.jastp.2006.08.011, 2007.

Moore, T. E. and Horwitz, J. L.: Stellar ablation of planetary atmospheres, Reviews of Geophysics, 45, 3002–+, doi:10.1029/2005RG000194, 2007.

Moore, T. E., Lundin, R., Alcayde, D., André, M., Ganguli, S. B., Temerin, M., and Yau, A.: Source processes in the high-altitude ionosphere, Space Sci. Rev., 88, 7–84, 1999.

Nilsson, H., Yamauchi, M., Eliasson, L., Norberg, O., and Clemmons, J.: The ionospheric signature of the cusp as seen by incoherent scatter radar, J. Geophys. Res., 101, 10 947–10 963, 1996.

Nilsson, H., Waara, M., Arvelius, S., Marghitu, O., Bouhram, M., Hobara, Y., Yamauchi, M., Lundin, R., Rème, H., Sauvaud, J.-A., Dandouras, I., Balogh, A., Kistler, L. M., Klecker, B., Carlson, C. W., Bavassano-Cattaneo, M. B., and Korth, A.: Characteristics of high altitude oxygen ion energization and outflow as observed by Cluster; a statistical study, Ann. Geophys., 24, 1099–1112, 2006.

Norqvist, P., André, M., Eliasson, L., Eriksson, A. I., Blomberg, L., Lühr, H., and Clemmons, J. H.: Ion cyclotron heating in the dayside magnetosphere, J. Geophys. Res., 101, 13 179–13 194, doi:10.1029/95JA03596, 1996.

Norqvist, P., André, M., and Tryland, M.: A statistical study of ion energization mechanisms in the auroral region, J. Geophys. Res., 103, 23 459–23 474, 1998.

Northrop, T. G.: The adiabatic motion of charged particles, Interscience Publishers, N.Y., 1963.

Parks, G.: Physics of space plasmas, an introduction, Addison-Wesley, Redwood City, CA, 1991.

Rème, H., Aoustin, C., Bosqued, J. M., Dandouras, I., Lavraud, B., Sauvaud, J. A., Barthe, A., Bouyssou, J., Camus, T., Coeur-Joly, O., Cros, A., Cuvilo, J., Ducay, F., Garbarowitz, Y., Medale, J. L., Penou, E., Perrier, H., Romefort, D., Rouzaud, J., Vallat, C., AlcaydE, D., Jacquey, C., Mazelle, C., d'Uston, C., Möbius, E., Kistler, L. M., Crocker, K., Granoff, M., Mouikis, C., Popecki, M., Vosbury, M., Klecker, B., Hovestadt, D., Kucharek, H., Kuenneth, E., Paschmann, G., Scholer, M., Sckopke, N., Seidenschwang, E., Carlson, C. W., Curtis, D. W., Ingraham, C., Lin, R. P., McFadden, J. P., Parks, G. K., Phan, T., Formisano, V., Amata, E., Bavassano-Cattaneo, M. B., Baldetti, P., Bruno, R., Chionchio, G., Lellis, A. D., Marcucci, M. F., Pallocchia, G., Korth, A., Daly, P. W., Graeve, B., Rosenbauer, H., Vasyliunas, V., McCarthy, M., Wilber, M., Eliasson, L., Lundin, R., Olsen, S., Shelley, E. G., Fuselier, S., Ghielmetti, A. G., Lennartsson, W., Escoubet, C. P., Balsiger, H., Friedel, R., Cao, J.-B., Kovrazhkin, R. A., Papamastorakis, I., Pellat, R., Scudder, J., , and Sonnerup, B.: First multispacecraft ion measurements in and near the Earth's magnetosphere with the identical Cluster ion spectrometry (CIS) experiment, Ann. Geophys., 19, 1303–1354, 2001.

Retterer, J. M., Chang, T., Crew, G. B., Jasperse, J. R., and Winningham, J. D.: Monte Carlo modeling of ionospheric oxygen acceleration by cyclotron

resonance with broad-band electromagnetic turbulence, Physical Review Letters, 59, 148–151, doi:10.1103/PhysRevLett.59.148, 1987.

Rönnmark, K.: Waves in homogeneous, anisotropic multicomponent plasmas (WHAMP), Tech. rep., 1982.

Seki, K., Elphic, R. C., Hirahara, M., Terasawa, T., and Mukai, T.: On atmospheric loss of oxygen ions from Earth through magnetospheric processes, Science, 291, 1939–1941, 2001.

Shelley, E., Johnson, R. G., and Sharp, R. D.: Satellite observations of energetic heavy ions during a geomagnetic storm, J. Geophys. Res., 77, 6104, 1972.

Waara, M., Slapak, R., Nilsson, H., Stenberg, G., and André, M.: Statistical evidence for $O^+$ energization and outflow caused by wave-particle interaction in the high altitude cusp and mantle, submitted to Annales Geophysicae, 2010.

Yau, A. W. and André, M.: Sources of ion outflow in the high latitude ionosphere, Space Sci. Rev., 80, $1 - 25$, 1997.

Zeng, W., Horwitz, J. L., Elliott, H. A., and Moore, T. E.: Simulation of the POLAR-observed Geomagnetic Ion Energy Spectrometer, Journal of Geophysical Research (Space Physics), 111, A12 215, doi:10.1029/2006JA011927, 2006.

**Institutet för rymdfysik**
Swedish Institute of Space Physics

**IRF**